# POLYMER DIELECTRICS FOR CAPACITOR APPLICATION

## 1. Introduction

The term dielectric was first used by Michael Faraday in the early 1800s to describe a phenomenon he observed when an insulator material was placed between two parallel plates of a capacitor. As an electric field is applied to the metal plates, the dielectric material between them becomes polarized to store electrical charge. Polarization can manifest in various ways, including electronic, ionic, and dipolar. An in-depth mathematical treatment of this topic is covered in several books on solid-state physics and dielectric theory (1,2). Polymers have gained prominence as dielectric materials due to their lightweight, low cost, graceful failure mode, and ease of processing (3). Several different polymers are used in dielectric applications, most notably polyethylene (PE) in extruded cables and biaxially oriented polypropylene (BOPP) for thin-film capacitor applications.

Besides polymers, inorganic materials such as ceramics have been used for capacitors applications due to their extremely large dielectric constants, often times >1000. However, despite their high dielectric constants, inorganic capacitors suffer from a low breakdown strength and nongraceful failure mode. This causes capacitors made from ceramics to fail in medium-to-high fields and results in a low overall energy density. Therefore, even capacitors made from specialized ceramics such as barium titanate ($BaTiO_3$) with a dielectric constant of ~1700 or strontium titanate with a dielectric constant of ~2000 have worse energy densities than BOPP, which has a dielectric constant of just 2.2, for any application requiring large amounts of energy storage capacity (4). To overcome these constraints, an increased focus has emerged recently to produce a polymer with metal atoms bound to their backbone that could offer the high dielectric constant found in ceramics with the graceful failure and ease of processing found in polymer films (5). This article is intended to serve as an overview of polymer dielectrics for capacitor applications, covering the most common materials in commercial use and current research focused on discovering new polymers.

## 2. Capacitor Specification and Dielectric Theory

**2.1. Capacitor Components.** One of the simplest and fastest ways to store electrical energy is with a capacitor. For power converter/inverters, DC-link and EMI filter capacitors constitute 40% of the footprint and the second greatest cost element after solid-state switches. Emerging SiC switch technology will provide power density in the range of 30 kW/L relative to present Si-IGBT technology at 5 kW/L, but implementation of SiC-based technology depends on the availability of high energy density, high temperature capacitors. High temperature polymer film capacitors not only offer improved volumetric efficiency but also eliminate active cooling requirements. Such design flexibility at the inverter level will provide hybrid system design engineers more efficient inverters that offer greater packaging flexibility for automotive manufacturers, thereby accelerating vehicle electrification, and will be transformative in the electric power industry in both power generation/distribution (smart-grids, etc) and consumption (PWM-based drives, distributed energy storage, etc). High performance capacitors
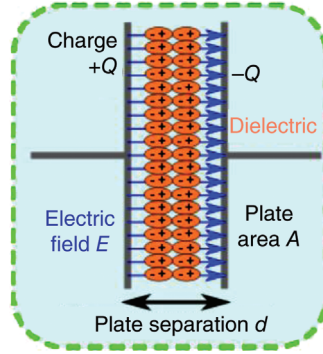
**Fig. 1.** A parallel plate capacitor diagram from the Ref. 7.

will facilitate deeper Oil & Gas wells and improve efficiency of electronics for aviation, aerospace, power electronics for renewable integration, transportation, combat vehicles, and directed energy weapons.

In its most basic form, a capacitor consists of two parallel, conductive plates separated by an insulating layer called a dielectric, as shown in Figure 1. Capacitors can be charged substantially faster than conventional batteries since there are no chemical reactions taking place and they can be cycled tens of thousands of times with a high efficiency without degradation (6). The electric charge that can be stored between the two parallel plate terminals follows the formula

$$C = Q/V$$

where $Q$ is the charge, $C$ is the capacitance, and $V$ is the electric potential. The dielectric material has the ability to store charges through various polarization processes and then hold these charges for long durations before they are released to loads at fast rate of millisecond to microseconds. Capacitors store electrostatic energy, given by $\frac{1}{2}CV^2$ within a dielectric between the two terminals. Between the conducting plates any insulator from paper impregnated with dielectric fluid to specialty polymers can be used in modern capacitors. Capacitance is followed by the equation

$$C = \varepsilon_r \varepsilon_0 A/d$$

where $\varepsilon_r$ is the relative dielectric permittivity of the capacitor, $C$ is the capacitance (Farad), $d$ is the thickness of the sample (m), $\varepsilon_0$ is the permittivity of free space $(8.854 \times 10^{-12}\,\text{F/m})$, and $A$ is the capacitor electrode surface area $(\text{m}^2)$ (8). Dielectric permittivity is actually a tensor and can be calculated from the measured capacitance using the above equation under a range of frequencies. Under an AC field, the complex permittivity of a material can be represented by an equation as

$$\varepsilon^* = \varepsilon' - j\varepsilon''$$

where $\varepsilon'$ and $\varepsilon''$ are the real and imaginary parts of the complex permittivity and $j = \sqrt{-1}$. The magnitude of $\varepsilon'$ and $\varepsilon''$ depend on the frequency of the applied electric

field. The real part of the permittivity can be expressed as

$$\varepsilon' = \varepsilon_{\mathrm{r}}\varepsilon_0$$

The imaginary part $\varepsilon''$ is correspond to the dielectric loss, and as the polarization of the dielectric material changes due to the applied electric field, some of the energy can be dissipated by to conduction (charge migration) or heat (thermal energy) as dielectric loss, which needs to be minimized as much as possible to have the maximum efficiency of the material.

The volumetric capacitance relates directly to the dielectric constant, while the energy density of a capacitor is determined by the dielectric constant. The dielectric constant has a linear relationship with energy density ($U_{\mathrm{e}}$), an increase in the dielectric constant increases the charge that can be stored between the capacitor plates shown in the following equation, where $\varepsilon'$ is the dielectric constant, $\varepsilon_0$ is the vacuum permittivity, and $E$ is the voltage of the applied electric field. To determine the maximum theoretical energy density of a material, $E$ is taken as the maximum field before breakdown occurs.

$$U = \frac{1}{2}\varepsilon_{\mathrm{r}}\varepsilon_0 E^2$$

In general, thin-gauge film capacitor is preferred due to volumetric effectiveness of voltage rating and strong thickness dependence of dielectric strength (9).

**2.2. Polarization and Relaxation.** Dielectric materials, in this case polymer dielectrics, are electrical insulators that can be polarized from its equilibrium or settled position by an applied electric field unlike conductor where charges flow through the materials. Polymers can only slightly shift from their average equilibrium positions causing dielectric polarization and as a result positive charges are displaced toward the applied electric field and negative charges shift in the opposite direction. If a dielectric material is placed in an electric field, a field is induced in the material that opposes the applied field.

Polarization includes electronic, ionic, orientational (or dipolar), and interfacial (10). Each polarization is connected with a dielectric loss at a specific frequency. For a given material, the net polarization is the summation of all the polarizations applicable for the specific system at the target frequency. Dipoles in the polymers can be arranged in different dipole and domain structures, as shown in Figure 2, which has close relationship with the charge–discharge phenomenon of dielectric materials (10).

If the molecules already possesses permanent dipole moments, as is the case in polymers, the dipoles will be aligned by the applied electric field to give a net polarization. This is the dipolar polarization. For polymers, dipolar relaxation usually takes place approximately between a fraction of 1 Hz and 100 MHz, depending on the nature of dipoles, phase transitions, and temperature. When the frequency becomes higher, dipolar polarization can no longer follow the oscillations of the electric field in the microwave region, around $10^{10}$ Hz; vibrational polarization can no longer track the electric field past the infrared or far-infrared region around $10^{13}$ Hz; electronic polarization loses its response in the ultraviolet region around $10^{15}$ Hz (10). In the frequency region above ultraviolet,
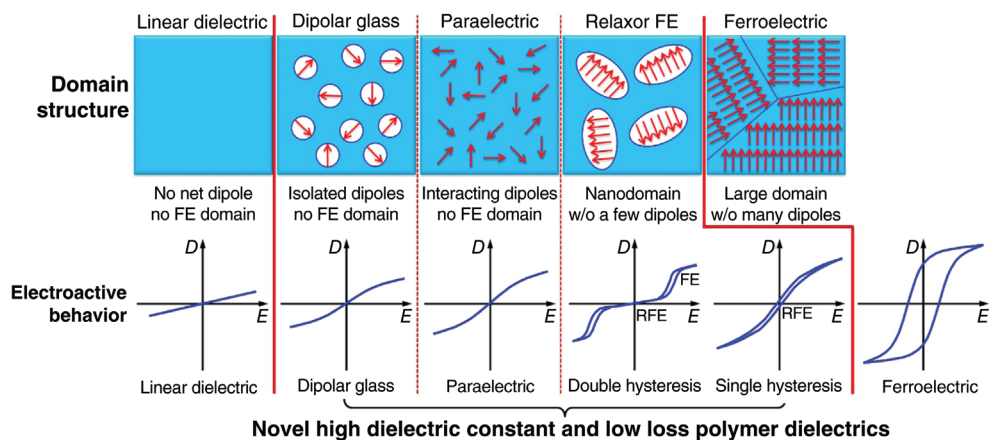
**Fig. 2.** Different dipole and FE domain structures with increasing dipole–dipole or domain–domain interactions from left to right (the top panel) and corresponding electroactive responses in $D$–$E$ loops (charge–discharge hysteresis loop) (the bottom panel) from the Ref. 10.

permittivity approaches the constant $\varepsilon_0$ in every substance, where $\varepsilon_0$ is the permittivity of the free space. Because permittivity indicates the strength of the relation between an electric field and polarization, if a polarization process loses its response, permittivity decreases. Since electronic polarization occurs in the visible region, it can be related to the refractive index ($n$) of the materials as follows, where $K_{\mathrm{elec}}$ is the electronic portion of the total dielectric constant ($\varepsilon'$) (5)

$$n = \sqrt{K_{\mathrm{elec}}}$$

Ionic transport in ionic conductor or ionic liquid used in electrical double-layer capacitors or batteries typically takes place in seconds to hours, due to low ionic mobility and the distributed $R$–$C$ time constants of the high surface area electrodes. When the dipoles experience friction as the result of collisions with other molecules, it results in increase in the temperature within the material, and hence dielectric loss occurs; this can be affected further by increasing temperature, humidity, and applied voltage as well.

## 3.  Traditional Polymer Dielectrics

Historically, kraft paper impregnated with mineral oil was used as dielectric films in capacitors. Polymer films gradually replaced the kraft paper because of their lower dielectric loss, high insulation resistance, good mechanical, thermal stability, and short production time. Some of the most common dielectric polymers (Fig. 3) and their properties are described in the following sections.

**3.1.  Polypropylene (PP).**   Until the early 1960s, kraft paper had been used as capacitor dielectric with pyranol impregnated dielectric fluid that provided low operating voltages (~300 V) with a loss factor an order of magnitude higher
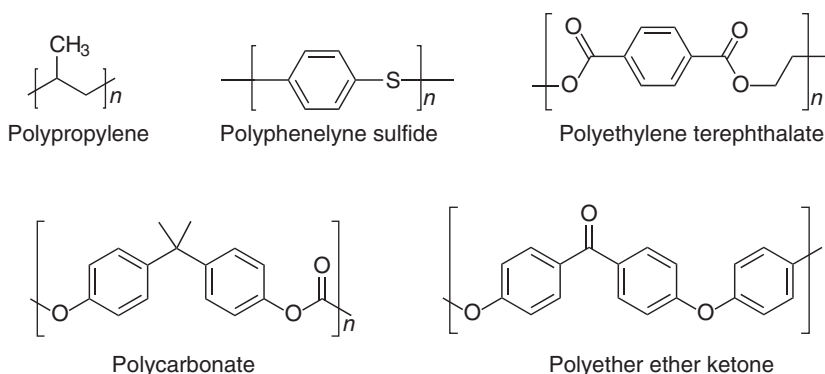
**Fig. 3.** Structures of some common polymers for thin-film capacitors.

than modern-day capacitors. Due to the limited applicability on thermal performance and material efficiency of kraft paper, it was replaced by BOP films. BOPP significantly reduced the volume and cost of capacitor production. However, it was reported that polypropylene was not resistant to chlorinated solvents and transformer oils. BOPP film has higher dielectric strength than the unoriented films by at least a factor of two due to the improvement of crystallinity within the films. BOPP has an extremely low dissipation factor of 0.0002 in an AC field, but this can be affected by impurities and contaminants leading to thermal runaway. Acceptable levels of impurities in the parts per million level and lower are acceptable depending upon the type of contaminants and capacitor application (11). The dielectric properties of BOPP are stable up to the operating temperature of 85°C and over a broad range of frequencies. This dielectric stability and low loss make this polymer a unique and widely used commercial dielectric material.

Isotactic polypropylene and atactic polypropylene have different morphological features and hence different dielectric constants. Isotactic polypropylene is highly crystalline and shows slightly higher dielectric constant (~2.28) compared with the relatively amorphous atactic polypropylene (~2.16). Higher loss occurs in atactic PP due to the higher polar impurities compared with isotactic PP that has rigid chain segments in the crystalline form hindering rotation. The polar impurity in nonpolar polymers is the unsaturation in the C—C double bond (~1–2%) from synthesis that is considered responsible for dielectric loss. This has been confirmed by infrared and other chemical analysis (12) (Table 1).

Other impurities such as residual catalyst, methyl side groups, polar end groups, dipoles arising from oxidation, the presence of antioxidant (additives), and processing residue can also affect the dielectric properties of PP. Dynamic mechanical studies suggest that two dielectric relaxation peaks are observed: a $\alpha$ peak at

Table 1.  **Properties of Polypropylene**

| Polymer | Density at 25°C (g/cm$^3$) | $\varepsilon'$ at 25°C | $\varepsilon''$(tan$\delta$) |
|---|---|---|---|
| isotactic PP | 0.912 | $2.28 \pm 0.04$ | 0.0002 |
| atactic PP | 0.865 | $2.16 \pm 0.07$ | 0.0010 |

Dielectric constant ($\varepsilon'$) and dielectric loss ($\varepsilon''$) data are shown for 1 kHz from the Ref. 12.

100°C due to amorphous phase and another peak β at room temperature due to the crystalline phase of the polymer. This β-phase is due to the fact that no polymer is 100% crystalline or amorphous. Isotactic PP can be highly crystalline due to its steric regularity, although it contains an amorphous phase since a few chain segments do not crystallize and can coexist with few atactic chains. Therefore, PP generally exhibits the characteristics of both phases. In the crystalline region, the polymer chain forms crystalline lamellae by ordering themselves to have regularity and stability. The amorphous segments have loose loops, tie chains, cilia, and randomly arranged as segregation and sometimes leading to branching. The interface domain between the crystalline and amorphous phases plays important roles in the overall morphological features of the polymers and, as a result, the electrical properties. The dynamic mechanical loss shows consistent behavior of this study, and suggests the semicrystalline nature of the isotactic rich amorphous phase. Acetone treatment can reduce the amorphous phase and extract the antioxidants from PP, decreasing the dielectric loss. The presence of antioxidants can cause high dielectric loss at higher temperature as well. Other impurities can cause conduction loss (13).

During the process of biaxially orienting the polymer film, the spherulite structures in the PP are deformed, elongated, and lose their crystalline identity in order to stack into microfibrils. This process of biaxially orienting can cause two different types of morphologies within the BOPP as either tenter or tubular types. The tenter structure exhibits a highly oriented crystalline phase connected with an extended and moderately oriented amorphous phase. The second type, tubular, has a network-like structure made up of crystalline zones and an amorphous zone that are not strongly oriented but are still in a slightly entangled state. Since the film is simultaneously oriented with a rather small orientation ratio, it exhibits residual flexural stiffness, constraints, and simultaneously distortion among amorphous chain. These structures are not strictly confined, rather they can be optimized by controlling the crystallization conditions, the draw ratios, and annealing temperature (14).

Polypropylene can be simultaneously cross-linked and degraded with UV irradiation that depends on the degree of crystallinity, for example, stereoregular PP cross-links to a lesser extent than PE (15). This premature aging has several disadvantages on insulation property of the material. Oxidative degradation, such as presence of reactive oxygen, atmospheric air, and gamma radiation, is the prominent cause of aging. They can incorporate new functional groups and structures, such as polar alcohol and carboxylic acids, within the polymer matrix, which eventually affect the dielectric behavior (16).

For high dielectric strength PP, high crystallinity, a small imbalance in orientation, and uniform film thicknesses are required. As previously stated, the fibrillated surface is required to promote complete impregnation by a dielectric fluid, and can be attained by the development of specific crystal morphology at one surface without any additives and control of impurities in the parts per million or parts per billion level (11).

**3.2. Polyphenylene Sulfide (PPS).**    PPS is a polymer with aromatic benzene ring with a sulfur atom in the main chain of the polymer. PPS is a high temperature engineering thermoplastic with a reported dielectric constant of 3.5. However, Frommer and co-workers suggest PPS behaves as an electrically

conducting material upon exposure to strong oxidizing agents. PPS is found to be semicrystalline and can be processed to be mostly amorphous, or it can be crystallized above its glass transition temperature ($T_g$). The amorphous phase relaxation peak at 100°C occurs at $10^5$ Hz in the amorphous material and a second relaxation peak (α relaxation) occurs at 140°C due to the semicrystalline content. Therefore, the fraction of relaxing dipoles increases with temperature and the relaxation time distribution shifts from ideal behavior to nonideal behavior as temperature increases (17). PPS is a good candidate for the replacement of polycarbonate (PC) dielectric films due to its outstanding chemical resistance, low water absorption (about 0.02%), excellent thermal stability (heat deflection temperature of greater than 260°C), high elastic modulus, and flame retardancy. PPS exhibits lower dielectric loss and equivalent dielectric properties compared with PC (18).

**3.3. Polyethylene Terephthalate (PET).**   PET is another widely used dielectric polyester for capacitor applications. PET is commercially synthesized by an ester exchange polymerization reaction between dimethyl terephthalate and ethylene glycol at temperature range from 195 to 280°C under atmospheric pressure with an excess of ethylene glycol. The process generally takes 2–5 h depending on the catalyst. Another synthetic route involves the direct reaction between ethylene glycol and terephthalic acid. While it is cost effective, the rate of the reaction is slow compared with the ester exchange reaction and it requires the removal of by-products and purification. The polymer produced by the later route exhibits poor ultraviolet light stability, poor hydrolytic stability, and is generally not suitable for film processing if the impurities exceed 10 mol% of the polymer (19). PET has good mechanical strength, chemical resistivity, and outstanding thermal stability (m.p. 260°C). This combination of properties lead it to be a good electrical insulating materials.

Relaxation processes caused either by the local movement of a specific molecule or by groups in the chain are called β, while the relaxation due to the movement of the whole chain is α. For PET, there are three different types of dielectric relaxation processes to be considered. The first relaxation process is correlated with mechanical and thermal properties of the polymer due to the relaxation of dipoles in the main polymer chain. The second is due to the presence of —OH groups, and the third relaxation that occurs at low frequencies and high temperatures is associated with the conduction of charges through the material. Generally, PET film shows β-relaxation in the range between –50 and 40°C that is attributed to the movement of ester groups with partial assistance of the phenyl group movement. The α-relaxation is situated in the range from 40 to 140°C with a peak at the temperature of 120°C. The ends of hydroxyl chains (—OH) and methylene units ($CH_3$) do not participate in the β-relaxation of PET. The α-relaxation results in much higher losses and gives rise to new configuration of the chain, causing changes of the dielectric and mechanical properties. The temperature of α-relaxation peak for PET is 120°C that is the glass transition temperature (20).

PET has dielectric constant ~3.3 over a broad range of frequencies. PET has significantly higher dielectric loss that increases with temperature and frequency compared with PP. Even though the energy density is 50% higher compared with PP, this variance in dielectric properties makes PET not a suitable option for high pulsed power applications. The biaxially stretched films with 68% degree of

crystallinity shows a phase transition at 160°C due to the conformational changes with melt transition. Polyethylene oxide (PEO), polycaprolactone (PCL), and silica ($SiO_2$) have been used with the PET films as a coatings to increase the electrical strength up to 10–15% and dielectric constant for 5 µm film thickness. However, the dielectric loss increases particularly at low frequencies (<10 Hz). For minimizing the loss, acrylate/barium titanate nanocomposites have been prepared and coated on PET. It also improves the dielectric strength and dielectric constant. This technique is recently being used in industrial production (18).

**3.4. Polycarbonate.**   PC was first developed in 1953 by Bayer in Germany, and General Electric in the United States. PC is known as a high performance engineering thermoplastics and environmentally friendly polymer due to its ability to be recycled. PC is most often synthesized from bisphenol A and phosgene by a step-growth polymerization in which $Cl^-$ ions are condensed. Bisphenol A contains two aromatic rings, which are responsible for its rigid structure. Due to its increased amorphous nature, the polymer is transparent. PC can be melt extruded to give pipes, and thin films. PC can also be injection molded to form specific parts computer and automotive applications.

PC film was first used in capacitor in the 1960s and since then it was successful for decades. PC has a dielectric constant of ~3 with an operational temperature from −55 to 125°C making it an attractive polymer for higher temperature applications than BOPP (21). In 2000, most suppliers had stopped producing polycarbonate film. One company, Electronic Concepts, still manufactures PC film in-house for their capacitors as of 2017. PC has a high impact strength below its $T_g$, which is due to the β-relaxation molecular motions of the main chain at low temperature. The broad β-relaxation peaks in PC are associated with more than one single relaxation process, one is for (the peak at lower temperature) relaxation of carbonate groups and the other (the peak at higher temperature) if for restricted motions of the phenyl groups (22). Limitations like large shrinkage, small Young's modulus, and easy formation of defects reduced its capacitor use, and PC has been replaced gradually with other polymeric dielectric films such as polyimide or polyphenylene sulfide (18).

**3.5. Polyether Ether Ketone (PEEK).**   PEEK is an ether-containing polymer where the backbone of the polymer contains ether linkages between aromatic groups. PEEK is synthesized by the step-growth polymerization with the disodium salt of hydroquinone and 4,4′-difluorobenzophenone in a polar aprotic solvent at high temperatures ~300°C. PEEK generally gives high molecular weight polymers and behaves as thermoplastic with good thermal stability. The crystalline/amorphous ratio in PEEK varies by selective annealing of the film in an inert atmosphere. It has high thermal and chemical stability, good mechanical properties, and a high glass transition temperature ($T_g$) making it a good choice for capacitor applications (23).

Investigations of PEEK performance at varying frequencies from 1 to 100 Hz and at different temperatures have found that dipolar orientation occurs at temperature regions of 100–180°C and ionic conduction occurs at 180–300°C. In the first temperature region, two phenomena are generally observed. The first is due to the dipolar relaxations associated with glass transition of the amorphous PEEK at 150°C, as shown in Figure 4. Second, above the $T_g$ there is an increase of the dielectric loss from 165 to 180°C. The second peak is due to the relaxation of the
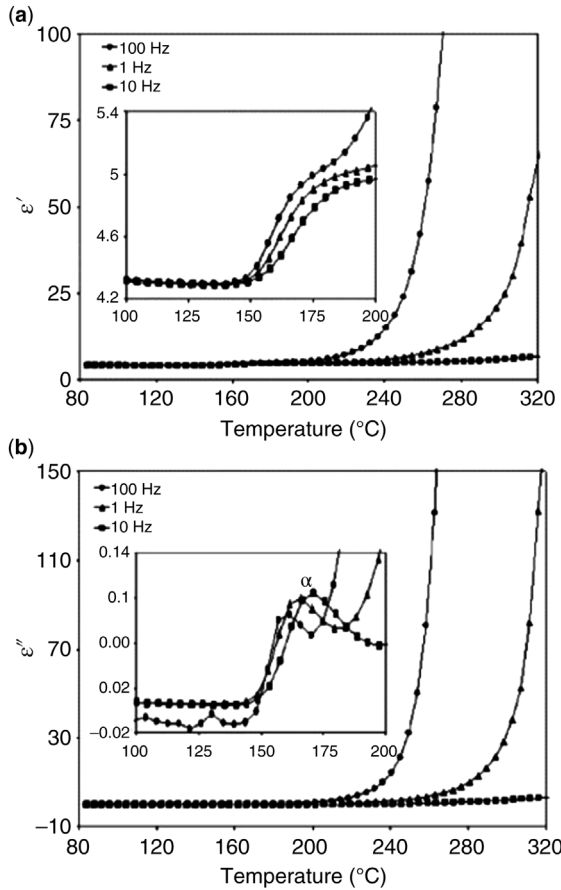
**Fig. 4.** (**a**) The dielectric constant ($\varepsilon'$) and (**b**) the dielectric loss ($\varepsilon''$) as a function of temperature for PEEK in three different frequency regions. (Reprinted with permission from Ref. 24. © 2007, Elsevier.)

just-crystallized sample whose amorphous part motions are restricted by the presence of crystals. In the higher temperature regions, the increase of permittivity due to ionic conduction is so dramatic that it masks the interfacial relaxation. The free volumes and defects at the crystalline/amorphous interface are potential contributors to breakdown. In the absence of other processing variables, there is a reduction in the dielectric breakdown strength as the morphology of the material changes from a purely amorphous nature to one of increasing crystallinity (24).
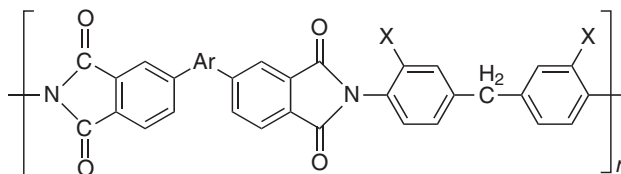
## 4. Next-Generation Dielectrics

Next-generation polymer dielectrics can be described as those not cheaply or currently mass produced due to their higher cost of materials or additional processing considerations. In general, the additional cost of the material is offset

by the additional benefits of the material, including higher operating temperatures, chemical resistivity, mechanical strength, adhesion, and many other properties. In recent years, there has been an emergence of interest to design new polymers with high energy density for pulse power applications. This work has predominantly been funded by a desire to shy away from weapons systems utilizing combustion, in the form of gunpowder and missiles, to eventually use electrically powered railguns and lasers (25,26). These military research initiatives bring added benefit to the civilian markets since the same polymer film capacitors can be used as DC-link capacitors for renewable energy generation and hybrid electric vehicles (27). To meet these growing needs, several strategies have emerged to increase the dielectric constant of polymers while keeping their losses low (10). Due to the vast number of potential polymers that could be synthesized and would need to be tested to select the best one, a rational codesign process was developed to synergistically carry out computational predictions, laboratory synthesis, and experimental property determination, to rapidly target promising polymer systems (28,29). Dielectric materials containing dipoles have grown recent interest due to their polarizability upon application of electric field. Materials containing dipole moment larger than 1.5 D (Debye) are able to achieve advanced dielectric performance such as high dielectric constant and low loss for high energy density capacitor applications (30). This section will outline some of the most promising polymers being developed, including polyimide, polyureas, polythioureas, polyurethanes, PVDF-based polymer systems, and organometallic polymers. Apart from the following polymers, there are a large class of inorganics, composites materials, and blended systems being explored depending upon the application for achieving better performance.

**4.1. Polyimide (PI).**    PIs are typically synthesized through step polymerization of a dianhydride and a diamine. Polyimides can be used as adhesives, films, moldings, fibers, membranes, foams, and coatings; further details on these can be found in several other books and entries. For electronic applications, polyimide films are of interest due to their aromatic nature leading to higher thermal stability that offers them to have high operation temperature compared with common polymers. Polyimides are attractive not only due to their high thermal stability but also for their radiation and chemical resistance, good mechanical strength, low moisture adsorption, and good adhesion to metal substrates.

Polyimides are of interest to replace silicone dioxide as insulating materials, for example, in semiconductors, printed microelectronics, and so on. Many of the polyimides previously synthesized are for either high dielectric constant high temperature applications or low dielectric constant material use. For low dielectric constants, this can be achieved by the modification of polymer backbone by lowering the polarizability. Also, bulky groups like aromatic phenyl group and use of fluorine instead of hydrogen can be effective in this goal by including more free volume inside the matrix and reducing the total polarizability by heightening the hydrophobicity (31). Previously, they are used for low dielectric constant containing microelectronics. Rigid aromatic polyimides are reported by Chisca and co-workers, as shown in Figure 5.

These polymers (PIa–PIf), shown in Figure 5, exhibit dielectric constants in the range of 2.78–3.48 and corresponding dielectric loss that is less than 2% overall at 1 kHz, as shown in Table 2. Polyimides with more bulky $CH_3$ (=X) groups show

PIa: Ar = –O–$C_6H_4$–C(CH$_3$)$_2$–$C_6H_4$–O– ; X = H
PIb: Ar = –O–$C_6H_4$–C(CH$_3$)$_2$–$C_6H_4$–O– ; X = CH$_3$
PIc: Ar = CO; X = H
PId: Ar = CO; X = CH$_3$
PIe: Ar = C(CF$_3$)$_2$; X = H
PIf: Ar = C(CF$_3$)$_2$; X = CH$_3$

**Fig. 5.** Structures of polyimides from the Ref. 32.

Table 2.   **Dielectric Constant and Loss Data for PIa–PIf at 1 kHz from the Ref. 32**

| Polyimide | $\varepsilon'$ (rt) | $\tan\delta$ (rt) |
|---|---|---|
| PIa | 3.25 | 0.0209 |
| PIb | 3.08 | 0.0293 |
| PIc | 3.48 | 0.0258 |
| PId | 3.32 | 0.0256 |
| PIe | 2.89 | 0.0202 |
| PIf | 2.78 | 0.0136 |

slightly lower dielectric constants compared with the similar structured polyimides of having H (=X) instead.

    In Figure 6, dielectric relaxation of PIb is shown as an example. A relaxation peak appears on dielectric loss spectrum in the negative temperature region
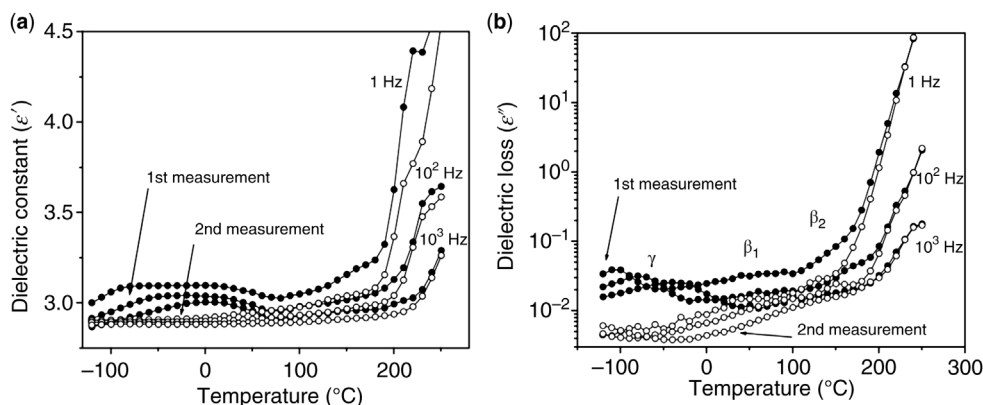


**Fig. 6.** Dielectric constant (**a**) and dielectric loss (**b**) as a function of temperature and frequency for polyimide PIb from the Ref. 32. (Reprinted with permission from IEEE. © 2011.)

referred as $\gamma$-relaxation, and a step increase in dielectric constant is observed and on the other hand after $50^\circ$C dielectric constant decreases with increasing temperature. At this temperature region, some irregular variation of dielectric loss occurs due to the removal of polar molecules like water. In the second heating, $\gamma$-relaxation is decreased and dielectric constant increases with temperature with two other subrelaxation processes ($\beta 1$ and $\beta 2$). At 150–200$^\circ$C, both dielectric constant and loss increase at low frequencies due the accumulation of charges at electrode sample interface. For PIs, the $\sigma$-relaxation peaks occur at the following temperatures: PIa 210$^\circ$C, PIb 210$^\circ$C, PIc 145$^\circ$C, PId 205$^\circ$C, at 1 Hz. For the polyimides PIe and PIf, $\sigma$-relaxation temperature is higher than 250$^\circ$C (32).

Dielectric constant of polyimides can be tuned and increased through increasing the amount of dipoles and dipole strength within the polymer. One such way to improve the dielectric constant is explored by incorporating very polar nitrile groups into the diamine backbone. Wang and co-workers synthesized a series of three novel ether linked aromatic nitrile diamines and polymerized them with four different aromatic dianhydrides, namely, pyromellitic dianhydride (PMDA), 3,3′,4,4′-benzophenone tetracarboxylic dianhydride (BTDA), 4,4′-oxydiphthalic anhydride (OPDA), and 4,4′-hexafluoroisopropylidene diphthalic anhydride (6FDA). These novel nitrile-containing polyimides exhibited $T_g$ values above 200$^\circ$C with degradation temperatures around 500$^\circ$C. It was found that the rotating aromatic nitrile dipole helped maintain the dielectric properties at various temperatures. The dielectric properties of these polymers were stable at both low ($-150^\circ$C) and high (190$^\circ$C) temperatures for use in power conditioning aerospace applications (33).

Recently, Ma and co-workers synthesized several polyimides with the help of Density Functional Theory (DFT) computations as a newly evolved rational codesign concept and characterized them for dielectric applications. Four different rigid aromatic dianhydrides, namely, PMDA, BTDA, OPDA, and 6FDA, along with two flexible diamines with aliphatic chains of different lengths, propane-1,3-diamine (DAP), hexane-1,6-diamine (HDA), JEFFAMINES D230, and JEFFAMINES HK511 were chosen as monomers (34) (Fig. 7).

These polyimides exhibit high dielectric constant due to their dipolar polarizability of the imide functional group. BTDA-HK511 films have the highest dielectric constant of 7.8 associated for the orientational polarization by the polyether segments along with lowest dielectric loss ~0.5% with operation temperatures limit up to 75$^\circ$C. Their properties are listed in Table 3.

For BTDA-HK511 dielectric constant decreases with increasing frequency due to slower orientation of the dipoles with alternating electric fields, while the dielectric loss increases due to chain relaxations. The breakdown field of BTDA-HK511 is 676 MV/m giving a maximum energy density 15.77 J/cm$^3$, although the highest breakdown field is found in BTDA-HDA of 812 MV/m with lower dielectric constant 3.57 compared with previous one. High quality film can be processed from BTDA-HDA and also with BTDA-HK511 polyimides (34). Currently, polyimides are seen as a favorable candidate for high temperature dielectric applications due to their thermal stability.

**4.2. Polyureas (PU).** Aromatic polyurea (ArPU)- and polythiourea (ArPTU)-based polymers are of interest due to their dipole moments of 4.5 and 4.89 D, respectively, and have higher dielectric constants than most of the
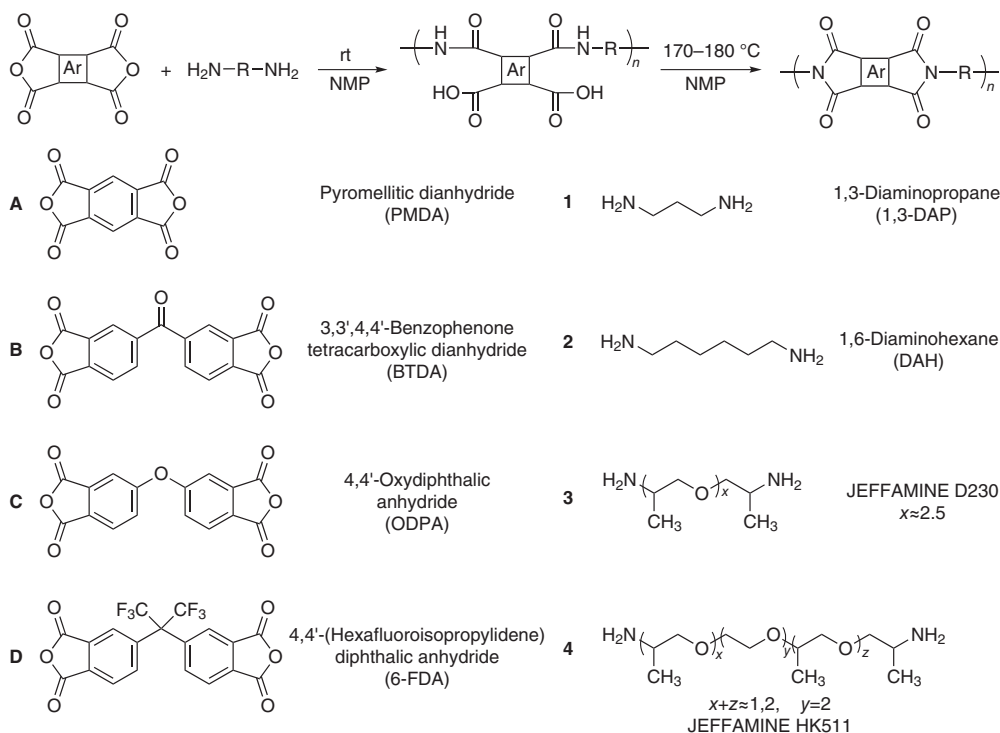
**Fig. 7.** Monomers and syntheses of polyimides A1–D4 from the Ref. 34.

traditional linear polymer dielectrics (35). Polyureas contain urea groups in their chain and can be synthesized by the reaction of diisocyanate and diamine, carbon dioxide (36), phosgene, urea derivatives, and water (37,38). Different techniques are available for synthesizing polyureas such as direct polymerization, solution polymerization, emulsion polymerization, and chemical vapor deposition polymerization. Linear polyureas are thermoplastic polycondensation products with aliphatic or aromatic structures. Aromatic polyureas have higher thermal stability compared with aliphatic polyureas. Polyureas were first commercialized at I.G. Farben, employing the reaction between diisocyanate and diamines. Some common monomers used in polyurea synthesis are shown in Figure 8.
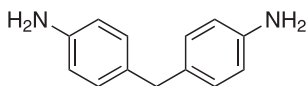
PU films are used for high energy density capacitors, especially under high temperatures (40). Aromatic polyureas are processable for thin-film capacitor applications. High purity dielectric films are synthesized by fabrication through

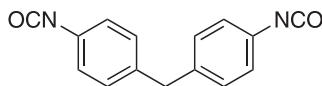Table 3.  **Properties of Polyimide A1–D4**

| Polyimide | B1 | B2 | A3 | A4 | B3 | B4 | C3 | C4 | D3 | D4 |
|---|---|---|---|---|---|---|---|---|---|---|
| $\varepsilon'$ (rt) | 4.01 | 3.57 | 4.17 | 5.44 | 4.52 | 7.80 | 4.37 | 6.04 | 2.50 | 5.26 |
| $\tan\delta$ (rt) | 0.255 | 0.849 | 0.518 | 0.660 | 0.256 | 0.555 | 0.166 | 0.714 | 1.47 | 0.791 |
| $E_g$ (eV) | 3.79 | 3.42 | 3.48 | 3.39 | 3.50 | 3.48 | 3.62 | 3.58 | 3.98 | 3.93 |
| $T_d$ (°C) | 498 | 482 | 458 | 450 | 452 | 447 | 465 | 461 | 453 | 452 |

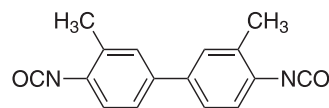Dielectric constant ($\varepsilon'$) and loss ($\tan\delta$) are presented for 1 kHz from the Ref. 34.
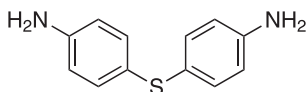
4,4'-Diaminodiphenylmethane (MDA)
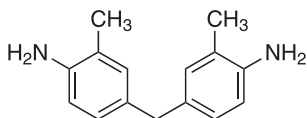
4,4'-Diphenylmethanediisocyanate (MDI)

4,4'-Diaminodiphenylether (ODA)

3,3'-Dimethyldiphenyl-4,4'-diisocyanate (MeDI)

4,4'-Diaminodiphenylsulfide (SDA)

4,4'-Diamino-3,3'-dimethyldiphenylmethane
(MeMDA)

**Fig. 8.** Typical monomers for polyurea from the Ref. 39.

vapor deposition polymerization (40). In this process a combination of an aromatic diamine [$H_2N$—$Ar_1$—$NH_2$] and an aromatic diisocyanate [OCN—$Ar_2$—NCO] monomers are vaporized under vacuum and coated on the surface of a substrate where they are adsorbed and react to give a copolymer of the general composition [—HN—$Ar_1$—NH—CO—NH—$Ar_2$—NH—CO—] (40). Thin film of thickness 500 nm is possible by this technique. Vapor deposition of 4,4′-diaminodiphenyl-methane (MDA) and 4,4′-diphenylmethane diisocyanate (MDI) on polyimide film substrate shows dielectric constant at 10 Hz 10 and 3.5 for MDA and MDI rich films, respectively. The dielectric constant increases with increasing temperature with loss less than 1% (41). The films of $p$(MDA–MDI) can reach a breakdown field about 800 MV/m. Higher energy density about 12 J/cm$^3$ at 800 MV/m with an efficiency of 95%, similar to BOPP. This energy density is stable over a broad temperature range from room temperature to 200°C. Both energy density and efficiency drop above 600 MV/m and temperature above 150°C. This is mainly due to the high conduction current under the high field and high temperature (41).

Recently, a structure property relationship with dielectric constant and dielectric loss in a series of polyurea thin films have been reported guided by DFT calculations. It was reported that dielectric constants greater than 4 were achieved from the rationally synthesized PU polymers. All-trans single polymer

Table 4.   **The Dielectric Constant ($\varepsilon'$) and Dielectric Loss (tan$\delta$) of the Polyureas at 1 kHz at Various Temperatures Along With Degradation Temperature ($T_d$) and Number Average Molecular Weight ($M_n$) of the Corresponding Polymers**

| Polyureas | $\varepsilon'$ (rt) | $\varepsilon'$ (100°C) | tan$\delta$ (rt) | tan$\delta$ (100°C) | $T_d$ (°C) | $M_n$ (g/mol) |
|---|---|---|---|---|---|---|
| PU1 | 5.18 | 5.85 | 0.0076 | 0.0539 | 246 | n/a |
| PU2 | 4.29 | 5.13 | 0.0089 | 0.0675 | 234 | n/a |
| PU3 | 3.47 | 3.38 | 0.0173 | 0.0124 | 227 | 37,500 |
| PU4 | 2.08 | 2.11 | 0.0312 | 0.0242 | 263 | 31,400 |
| PU5 | 6.19 | 6.87 | 0.0429 | 0.0444 | 264 | 29,100 |

rt, room temperature.
*Source*: Reprinted with permission from Ref. 42. © 2013, Elsevier.

chain containing four independent blocks with periodic boundary conditions along the chain axis are considered here. The dielectric constant systematically increases and the dielectric loss decreases as the number of carbons between polarizable functional groups decreases. Therefore, an increase in free volume within the polymer matrix decreases the number of polarizable groups per unit volume and decreases the overall dielectric constant, as shown in Table 4 (Fig. 9).

These polymers have high thermal stability with degradation temperature above 220°C. They do not exhibit any glass transition temperature below their melting temperature. Melting temperature ranges from 201 to 241°C. Number average molecular weight ranges from 29,000 to 37,000 g/mol with a PDI between 1.31 and 1.45. The introduction of an ether moiety in the polymer repeat units significantly increases the dielectric constant, as shown in Table 3. The dielectric loss (tan$\delta$) has the inverse trend as smaller alkyl spacers results in lower dielectric loss.

Another class of polyurea, namely, *meta*-aromatic polyurea (*meta*-PU), has higher energy density and improved dielectric constant. Dipolar density and dipole moment can be tuned with this modified *meta*-PU. Higher volume of dipolar density is achieved by the green synthesis of *m*-phenylenediamine and diphenyl carbonate, as shown in Figure 10. It has a dielectric constant of 5.6, higher than aromatic PU, due to the increased volume dipole density $N$ in the *meta*-PU repeat unit with a dielectric loss at low field (<10 MV/m) about 1.5% from 100 Hz to 1 MHz frequency range. It is thermally stable up to 160°C with no significant change in
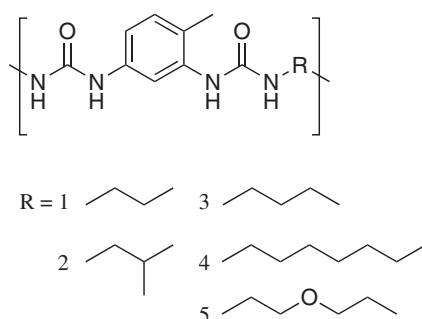


**Fig. 9.** Rationally designed polyureas (PU1-5) with varying R groups. (Reprinted with permission from Ref. 42. © 2013, Elsevier.)

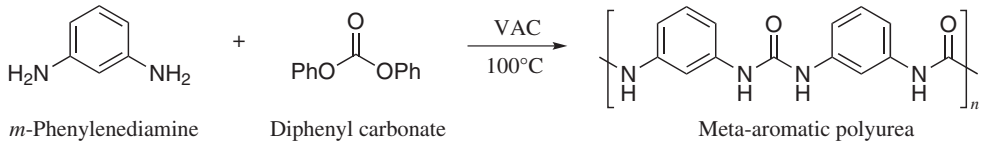m-Phenylenediamine          Diphenyl carbonate                    Meta-aromatic polyurea

**Fig. 10.** Synthetic route of *meta*-PU from the Ref. 43.

the dielectric constant and loss from 30 to 160°C. Energy density of *meta*-PU is 13 J/cm$^3$ with 91% energy storage efficiency and 670 MV/m breakdown strength (43).

**4.3. Polythioureas (PTU).**   A linear polythiourea is synthesized by the polycondensation of thiourea with formaldehyde to achieve the simple structure —NH—CS—NH—CH$_2$—, or the reaction of a diamine with carbon disulfide, thiophosgene, or diisothiocyanate. Aromatic polythiourea (ArPTU) is an amorphous, polar, glass-phase dielectric polymer. It is to be noted that thiourea has a chemical structure H$_2$N—CS—NH$_2$, in which the amino group is electron-donating and CS is electron-withdrawing giving an overall dipole moment of ~4.89 D. It behaves as organic ferroelectric due to its spontaneous polarization and ferroelectric behavior. The first work on polythiourea as a ferroelectric polymer was published in 1978 when Ohishi and co-workers synthesized aliphatic polythiourea by condensation reaction of diamine with carbon disulfide with varying chain length of aliphatic spacers. This work proves that these polymers possess hydrogen bonding due to their highly polar nature. The amount of hydrogen bonding can be controlled by molecular design of chemical structure, which eventually affects the dielectric relaxation of polythioureas.

An ArPTU of 4,4′-diphenylmethanediamine (MDA) with thiourea in NMP by microwave-assisted polycondensation has reported to have an ultrahigh energy density (~22 J/cm$^3$), low dielectric loss at high fields and high breakdown strengths (~1 GV/m), and molecular weight of ~8,000–12,000 g/mol. This polymer is reported by Shan Wu and co-workers and shown in Figure 11 with a comparison of the ArPTU to BOPP. The high breakdown field of polar amorphous polymer is due to the presence of random dipoles in an amorphous structure that provide substantially stronger scattering to charge carriers. The limitations of this polymer are its inability to form freestanding films primarily due to its low molecular weight (44).

Recently, a new set of aromatic polythiourea is synthesized and characterized for capacitor dielectric applications, shown in Figure 12, with the help of DFT computation. The dielectric constants, bandgap energies ($E_g$), dielectric loss (tan$\delta$), number average molecular weight ($M_n$), degradation temperature ($T_d$), and breakdown strengths are listed in Table 5. Dielectric constant for PDTC-HK511 shows highest among others due to its flexible polar oxygen group inside the repeat unit. The bandgap provides a good proxy for the dielectric breakdown field strength since a higher bandgap would imply a higher threshold for impact ionization. The ability to operate at high electric fields leads to a significant increase in energy density. PDTC-HDA has high energy density of 9.3 J/cm$^3$ at a maximum applied field of 685 MV/m (45).
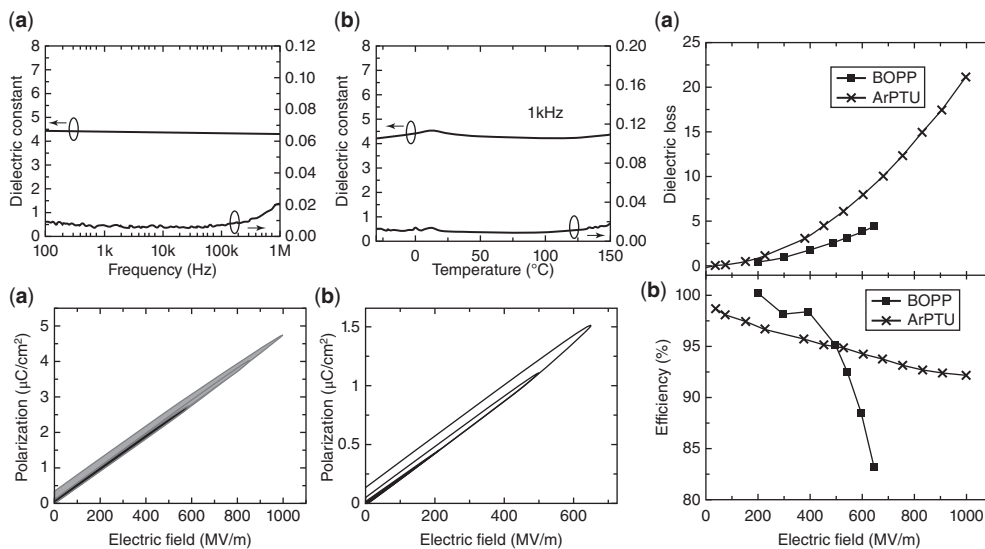
**Fig. 11.** *Top*: (**a**) Dielectric properties as a function of frequency at room temperature. (**b**) Dielectric properties at 1 kHz versus temperature of ArPTU films. *Bottom*: (**a**) *D–E* curves of the ArPTU films and (**b**) *D–E* curves of BOPP films under different applied fields at 10 Hz. *Right*: (**a**) Energy density of the ArPTU film compared with BOPP. (**b**) $\eta$ of the ArPTU film compared with BOPP (at 10 Hz). (Reprinted with permission from Ref. 44. © 2013, John Wiley & Sons, Inc.)

These new polymers exhibit low dielectric loss and high energy densities of ~10 J/cm$^3$. The variation of polymer backbone using aromatic, aliphatic, and oligoether segments allowed for tuning dielectric properties through introduction of additional permanent dipoles, conjugation, and better control of morphology. One notable example is PDTC-HDA with an energy density of 9.3 J/cm$^3$ with a breakdown strength of ~685 MV/m. Hysteresis observed in the *D–E* loops is attributed to conduction loss at high voltage due to the residual solvent and other impurities in the polymer film. The film casting conditions such as speed, drying condition, and thermal annealing can affect different surface morphology, which affects the breakdown voltage (45).

**4.4. Polyurethanes (PUR).** PUR has a carbamate (urethane) linkage inside their polymer repeat units. Both thermoplastic and thermoset polyurethanes are available. Generally, they are synthesized by the di- or polyisocyanate with a polyol or diol. The properties of a polyurethane are influenced by the types of monomer that has been used, for example, if long, flexible diols are used, then soft elastic polyurethane would form. When more than two functional group monomers are used, it can lead to rigid cross-linked polymers. There are two additional ways by which cross-linking is possible, through hydrogen bonds or submicroscopic phase separation of urethane-containing blocks in the main chain of polymer, which leads to dispersion of hard regions attached to matrix of rubbery material (46).

Polyethylene glycol-containing polyurethanes, such as polyethylene glycol 200 polyurethane, polyethylene glycol 600 polyurethane, and polypropylene glycol 450 polyurethane elastomer have been reported to exhibit low dielectric constants,
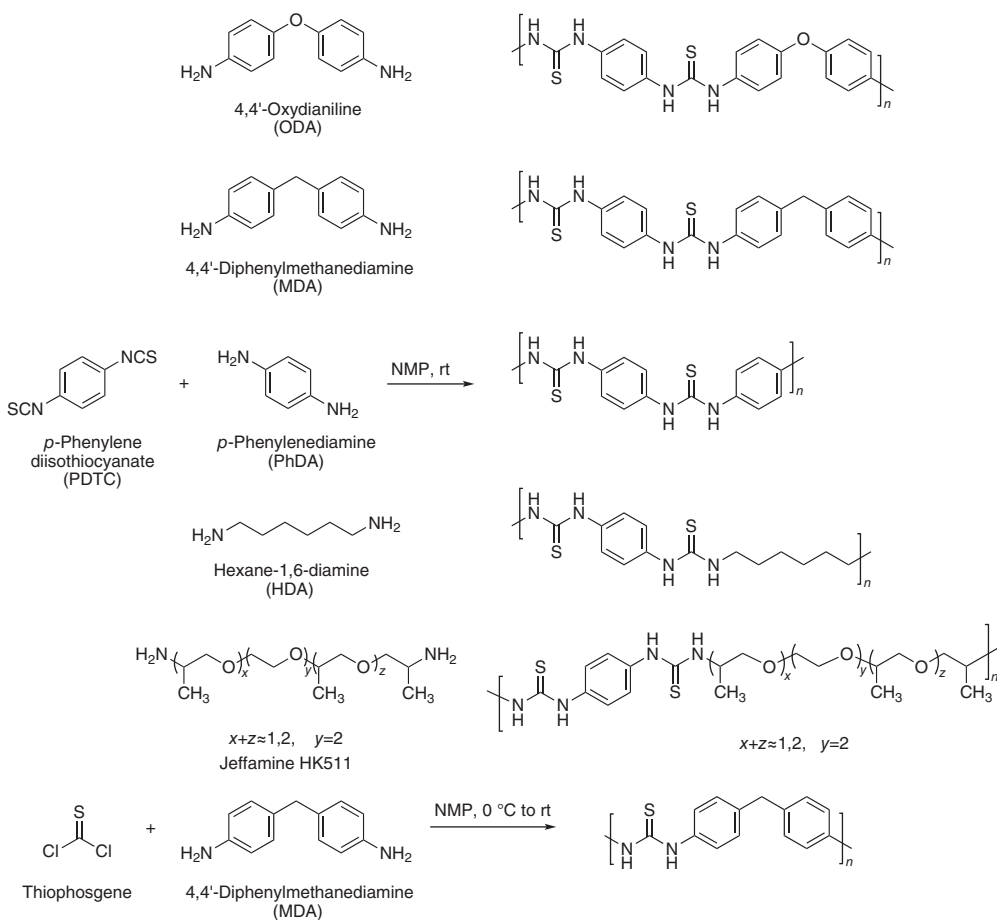
**Fig. 12.** ArPTU synthetic route and structures from the Ref. 45.

but they have low dielectric loss below their transition temperatures. Above the transition temperature high dielectric constant and high dielectric loss have been observed due to the introduction of a second phase with high interfacial polarization suggestive of a two-phase structure (47).

Table 5.  **Properties of ArPTU**

| Polymer | $\varepsilon'$ (rt) | $\tan\delta$ (rt) | $E_g$ (eV) | $M_n$ (g/mol) | $T_d$ (°C) | Breakdown field (MV/m) |
|---|---|---|---|---|---|---|
| PDTC-ODA | 4.52 | 0.0233 | 3.22 | 21,500 | 246 | 704 |
| PDTC-MDA | 4.08 | 0.0348 | 3.16 | 56,400 | 228 | 714 |
| PDTC-PhDA | 4.89 | 0.0144 | 3.07 | n/a | 276 | n/a |
| PDTC-HDA | 3.67 | 0.0267 | 3.53 | 85,100 | 275 | 666 |
| PDTC-HK511 | 6.09 | 0.0115 | 3.51 | 25,900 | 294 | 602 |
| thiophosgene-MDA | 3.84 | 0.0226 | 3.30 | 44,600 | 311 | 677 |

Dielectric constant ($\varepsilon'$) and dielectric loss ($\tan\delta$) presented here for 1 kHz along with bandgap energy ($E_g$), number average molecular weight of the polymer ($M_n$), degradation temperature ($T_d$), and breakdown field strength of the corresponding polymers.
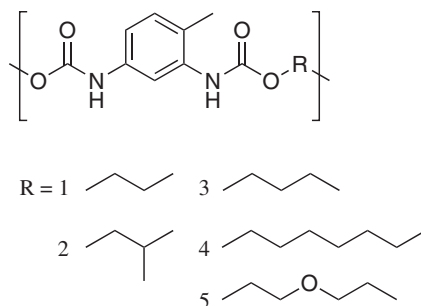*Source*: Reprinted with permission from Ref. 45. © 2013, Elsevier.

**Fig. 13.** Structure of polyurethanes.

Recently, a new series of polyurethane has been synthesized and characterized for the dielectric applications, as shown in Figure 13 and Table 6.

Polyurethanes exhibit higher dielectric constants compared with polyureas due to the higher electronegative oxygen atom (compared with nitrogen) in the repeat unit of polymer, which helps to improve the ionic polarizability. Here, similar situation observed as of polyureas with the number of aliphatic spacers reduce the dielectric constants of the material.

**4.5. Polyvinylidene Fluoride (PVDF).** PVDF, $(-CH_2-CF_2-)_n$, is a thermoplastic fluoropolymer synthesized by the polymerization of vinylidene difluoride via a free radical (or controlled radical) polymerization process. Later, the synthesized polymers are processed by melt casting, solution casting, spin coating, or film casting. The high purity PVDFs are stable in atmospheric conditions and unaffected by most common solvents, acids, and bases. PVDF-based materials are the most studied dielectric materials for their larger dielectric constant due to their ferroelectric nature. Ferroelectrics and antiferroelectrics have a close relationship in terms of their polarization process. In the ferroelectric materials, the adjacent dipoles in one domain have the same direction of polarization by the application of external electric field. On the contrary, in antiferromagnetic materials, the adjacent dipoles can be arranged in opposite direction and under very high field they can be rearranged and transformed into their ferroelectric state (48).

There are four different crystalline phases present in PVDF. The α-phase is the nonpolar crystalline phase that results from rapid cooling, while the rest are ferroelectric. The β-phase has the largest polarization due to the large dipole

Table 6. **Properties of Polyurethanes**

| Polyurethane | $\varepsilon'$ (rt) | $\varepsilon'$ (100°C) | $\tan\delta$ (rt) | $\tan\delta$ (100°C) | $T_d$ (°C) | $M_n$ (g/mol) |
|---|---|---|---|---|---|---|
| PUR1 | 6.35 | 8.43 | 0.0126 | 0.0650 | 237 | 24,300 |
| PUR2 | 6.74 | 6.74 | 0.0154 | 0.0140 | 251 | 19,600 |
| PUR3 | 5.81 | 5.63 | 0.0139 | 0.0608 | 251 | 28,700 |
| PUR4 | 4.09 | 4.37 | 0.0156 | 0.0220 | 277 | 21,700 |
| PUR5 | 10.5 | 12.0 | 0.0188 | 0.0615 | 249 | 37,900 |

Dielectric constant ($\varepsilon$) and dielectric loss ($\tan\delta$) data are presented for 1 kHz along with the degradation temperature ($T_d$) and number average molecular weight ($M_n$) of the corresponding polymers from the Ref. 42. © 2013, Royal Society of Chemistry.

moment. The γ-phase is formed by drying with a polar solvent below 100°C or by high temperature annealing. The δ-phase is induced by the application of an external electric field (100–200 MV/m) during the rapid cooling. These phases are important since they are closely related to the dielectric constant and energy density. For example, the γ-phase has the largest energy density 14 J/cm$^3$ compared with other three phases that are in the range of 1.5 J/cm$^3$ (7). Figure 14 depicts the room temperature dielectric results of three samples, A, B, and C, which were crystallized from solution at 60, 90, and 120°C with different proportions of the α- and β-phases. The increase in dielectric loss with frequency, observed in the high frequency regions, is due to the β-relaxation process associated with the glass transition of PVDF. There are two theories associated with this relaxation, one process refers as the micro-Brownian movement of the amorphous phase chain segments above the $T_g$ when the molecules have large mobility. The other process refers the movement of crystalline–amorphous interphase chain segments. This dipolar relaxation process accounts for the high dielectric constant of PVDF (49). PVDF in its three crystal forms have similar energy density and dielectric loss, such as α-phase of PVDF has the energy density of 300 MV/m; however, it
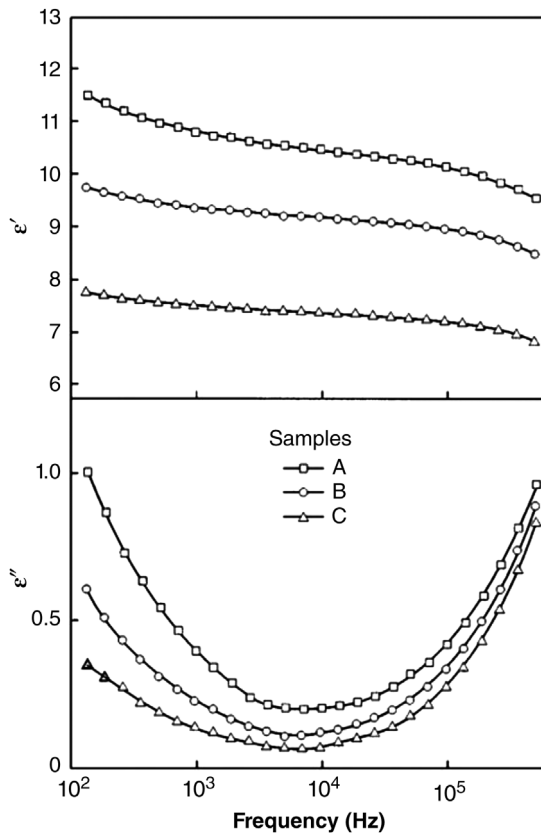


**Fig. 14.** Variation in $\varepsilon'$(dielectric constant) and $\varepsilon''$(tan$\delta$) with frequency for the samples crystallized from solution at 60°C (square), 90°C (circle), and 120°C (triangle). (Reprinted with permission from Ref. 49. © 1999, Springer.)

has higher loss than γ, which can withstand up to 200–350 MV/m. The quenched γ PVDF can withstand up to 350 MV/m with highest energy density 14 J/cm$^3$ (50).

PVDF and its randomized copolymer $p$(VDF-TrFE) with trifluoroethylene (TrFE) (CHF=CF$_2$) have also been widely known as ferroelectric materials for energy storage applications. Their prime limitation is their high remnant polarization that affects the energy density, which can be minimized by defect modifications. In copolymer of $p$(VDF-TrFE), 50–80 mol% of VDF ratios show ferroelectric transitions, in which TrFE moiety is considered as a defect. When increasing the amount of defects, the β-phase becomes less stable making them a tailorable ferroelectric materials. With the incorporation of defects, ferroelectric PVDF can be converted into relaxor ferroelectric polymers with small remnant polarization, which can give high electric displacement below its breakdown field, making it a high energy density dielectric materials. Copolymer of PVDF 70% and TrFE 30% makes them a ferroelectric relaxor upon irradiation under He gas at a dose rate of 2.5 MGy/h with beam energy 2.5 MeV, after which it exhibits a lower strain level compared with copolymers irradiated above 100°C (51).

Poly(vinylidene fluoride–trifluoroethylene–chlorotrifluoroethylene), P(VDF–TrFE–CTFE), and poly(vinylidene fluoride–trifluoroethylene–chlorofluoroethylene), P(VDF–TrFE–CFE), terpolymers containing CTFE (CClF=F$_2$) and CFE (CF$_2$=CF$_2$) comonomers, respectively, also have relaxor ferroelectric behavior such as diffuse phase transition, slim polarization hysteresis loop, and high dielectric constant at room temperature. They also show larger electrostrictive strain response than the irradiated copolymers. CFE and CTFE monomers act as molecular defects to mitigate the large ferroelectric domains of P(VDF–TrFE) into small domains that helps to make a slim hysteresis loop with high dielectric constant (>50) measured at 1 kHz near room temperature, the highest among all known polymer dielectrics near room temperature. Energy density of this P(VDF–TrFE–CFE) terpolymer is 10 J/cm$^3$ (51).

Two random copolymers of PVDF with chlorotrifluoroethylene (CTFE) and hexafluoropropylene (HFP) (CF$_3$—CF=CF$_2$) have been developed as P(VDF–CTFE) and P(VDF–HFP) to tune the dielectric constant to solve the problem of early electric displacement saturation. PVDF 91% and CTFE 9% containing copolymer shows energy density 17 J/cm$^3$ with breakdown field (>700 MV/m). With improved film quality reachable energy density can be 25 J/cm$^3$. On the other hand, P(VDF–HFP) defect incorporated copolymer with 10% HFP exhibits breakdown field (700 MV/m) and energy density (>25 J/cm$^3$) (48).

## 5. Computation-Driven Design of Polymer Dielectrics

Materials research has benefited significantly from the use of modern computational and data-driven methods. Traditional trial-and-error type approaches to materials design are increasingly being replaced by computation-guided experimental design. While the synthesis and testing of an enormous number of materials is impractical, both time and money can be saved by screening for potentially useful candidates *in silico*. In this section, we describe a rational design approach centered around high-throughput computations and targeted
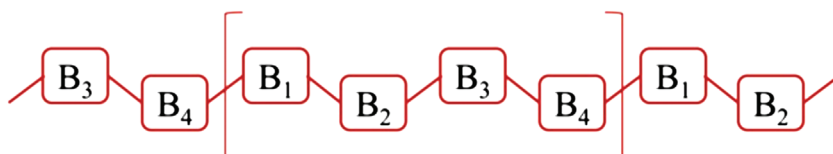
experimentation aimed at discovering new and advanced polymer dielectrics for energy storage capacitor applications.

Density functional theory (DFT) was chosen as the computational workhorse to study two crucial properties of known and novel polymers, the dielectric constant and the bandgap. These properties provide a useful initial screening criterion for capacitor dielectrics. High-throughput DFT (the term high-throughput implying the use of large computational resources on many materials over an extended period) led to the identification of several promising candidates, followed by their synthesis and characterization, thus validating the computations and providing new materials to potentially replace the state-of-the-art polymeric capacitor dielectric.

As a first step, appropriate DFT formalisms had to be determined for property computation. Density functional perturbation theory (DFPT) (52,53) is a powerful technique where the dielectric constant of a material is estimated by studying the system responses to applied electric fields. The bandgap can be computed accurately using the hybrid Heyd–Scuseria–ErnzerhofHSE06 electronic exchange-correlation functional (54,55), which corrects for the bandgap underestimation associated with standard DFT. Dielectric constants and bandgaps computed using DFPT and the HSE06 functional, respectively, have been shown to match up very well with experimentally measured results (8,29), and were thus chosen for performing the high-throughput DFT computations.

## 5.1. High-Throughput DFT on an Organic Polymer Chemical Space.

An organic polymer chemical space (shown in Fig. 15) consisting of seven basic building blocks – $CH_2$, NH, CO, $C_6H_4$, $C_4H_2S$, CS, and O – was selected for initial high-throughput computations. Any *n-block* polymer here was generated by linearly connecting *n* blocks with each of them drawn from the seven possibilities, and DFT calculations were carried out for approximately 300 *4-block* polymers (28,56). The ground state crystal structures were determined for all the polymers using a structure prediction algorithm known as Minima Hopping (57).

DFT was applied on the lowest energy structure of every polymer to compute the dielectric constants and bandgaps, which are plotted against each other in Figure 16. From DFPT, the dielectric constant is computed as two separate components: the electronic part, which depends on atomic polarizabilities, and the ionic part, which comes from the IR-active vibrational modes present in the system. The total dielectric constant is expressed as a sum of the electronic and the ionic parts. While the electronic dielectric constant appears to be constrained by



$$B_i \in \{NH, CO, C_6H_4, C_4H_2S, CS, O, CH_2\}$$

**Fig. 15.** The chemical subspace of polymers generated by linear combinations of seven basic chemical units. (Reprinted with permission from Ref. 29. © 2016, John Wiley & Sons, Inc.)
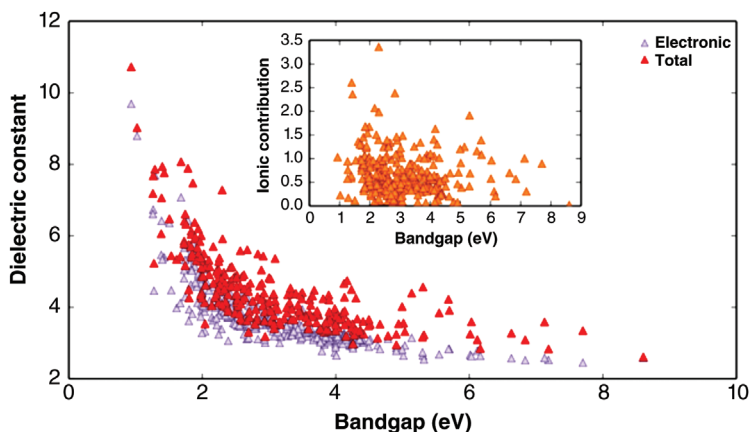
**Fig. 16.** The dielectric constants (divided into electronic and ionic parts) and bandgaps of 284 polymers computed using DFT.

some sort of an inverse relationship with the bandgap, the ionic dielectric constant shows little or no correlation with the bandgap. This effect translates to an inverse relationship between total dielectric constant and bandgap as well, given the larger range of values of the electronic part compared with the ionic part.

Although a wide spectrum of dielectric constant values ($\sim$2–12) and bandgap values ($\sim$1–9 eV) were covered by this chemical subspace of polymers, only roughly 10% of the total points populating the *high dielectric constant, large bandgap* region, defined by dielectric constant >4 and bandgap >3 eV. Three polymers belonging to three distinct polymer classes – polyurea, polyimide, and polythiourea – were selected from this region and synthesized in the laboratory (29). Appropriate monomers and reaction schemes were adopted here to yield satisfactory quantities of each polymer, following which ultraviolet–visible spectroscopy (UV–vis) was performed to estimate the bandgaps and time domain dielectric spectroscopy (TDDS) to measure the dielectric constants. The experimental results matched quite well with the computational results, providing not only a validation for the high-throughput DFT scheme but also three novel promising polymer dielectric candidates for energy storage capacitor applications (58).

However, it was seen that these initial polymers had solubility issues and could not be processed into thin films, which is an important capacitor dielectric requirement. To overcome these issues, newer, longer chain polymers belonging to the same and related polymer classes were synthesized and tested (31,34,42,45). Freestanding films were made from most of these polymers, and their dielectric constants, bandgaps, dielectric breakdown strengths, loss characteristics, and recoverable energy densities were experimentally measured. Among the best performing polymers thus realized were a polythiourea named PDTC-HDA, a polyimide named BTDA-had, and another polyimide named BTDA-HK511, where PDTC stands for *para*-phenylene diisothiocyanate, HDA stands for hexane diamine, BTDA stands for benzophenone tetracarboxylic dianhydride, and HK511 is a jeffamine-containing ether. Not only could freestanding films be formed, but each polymer displayed an energy density two to three times higher

than BOPP owing to higher dielectric constants and comparably high breakdown strengths.

Thus, new organic polymers were successfully designed that can potentially replace BOPP in capacitor applications. The rationale for pursuing these polymers came from computational guidance; however, the choice of the specific polymer repeat units was determined by the polymer chemists using their experience and knowledge of chemical feasibility, solvent considerations, and film formability. The experimental data thus obtained further bolster our knowledge of polymer dielectrics and provide vital leads on newer chemical blocks to introduce in polymers for future computational studies.

**5.2. Moving Beyond Pure Organics: An Organometallic Polymer Chemical Space.**   Given the lack of dependence of the ionic dielectric constant on the bandgap, it was suggested that the former could perhaps be enhanced without adversely affecting the latter. Studies carried out for the halides of group 14 elements showed that Pb-, Sn-, and Ge-based compounds have much higher dielectric constants than their C or Si counterparts, as well as bandgap values around or greater than 4 eV (59,60). Furthermore, it is known that metal-organic frameworks (MOFs) – compounds containing metal clusters surrounded by organic ligands – are commonly used for gas storage, catalysis, and supercapacitors (61). Based on these ideas, a metal-organic polymer framework was proposed where the organic polymer chain is interrupted by a metal-containing unit. For initial study, Sn was chosen as the metal atom, and polymer repeat units were generated by introducing tin fluoride ($-SnF_2-$), tin dichloride ($-SnCl_2-$), and dimethyltin ester ($-COO-Sn(CH_3)_2-COO-$) units in polyethylene chains in varying amounts (5,62–64). DFT calculations showed that these systems indeed display superior dielectric constants compared with organics for a given bandgap value; the Sn ester-based polymers were duly synthesized and tested. As shown in Figure 17, some of the organo-Sn polyesters showed extremely high dielectric constants of >6 for bandgaps >6 eV (Fig. 18).
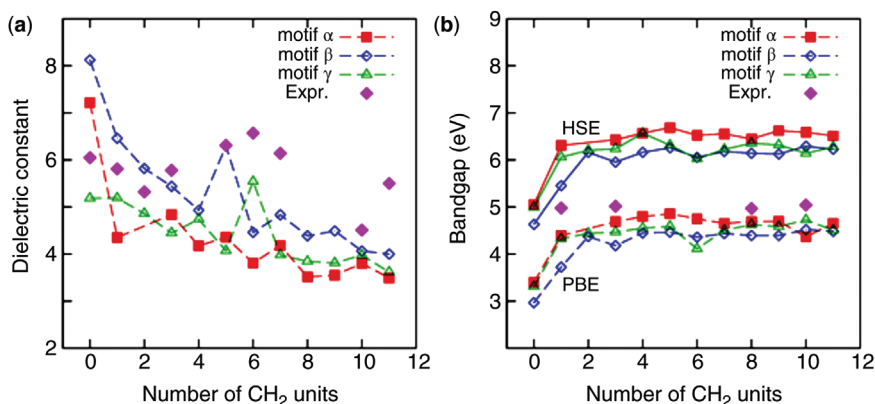


**Fig. 17.** Computational and experimental dielectric constants and bandgaps for a series of organo-Sn polyesters as a function of the number of linker $-CH_2-$ units. The DFT results are shown for three kinds of structural motifs – α, β, and γ. (Reprinted with permission from Ref. 47. © 2016, John Wiley & Sons, Inc.)
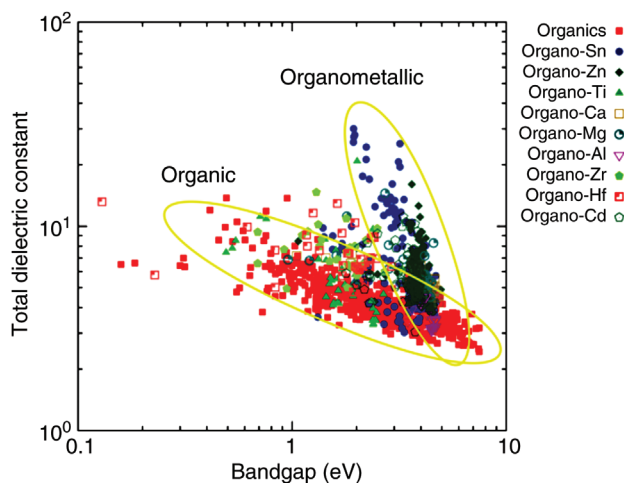
**Fig. 18.** DFT computed bandgaps and dielectric constants for all organic and organo-metallic polymers. The organometallics show higher dielectric constants than the organics for a given bandgap. (Reprinted with permission from Ref. 47. © 2016, John Wiley & Sons, Inc.)

The effects of amount of tin loading in the polymer repeat units by varying the length of the aliphatic spacers on properties such as low energy structural motifs, dielectric constants, dielectric loss, and energy bandgap are reported. This novel study suggests the increase in the dielectric constant by incorporation of metal atoms covalently bonded into the polymer backbone reduces and in some cases eliminates the dispersion difficulties such as agglomeration of particles observed in nanoparticles and nanocomposites. Poly(dimethyltin esters) are synthesized by the interfacial polymerization technique described by Zilkha and Carraher with some modification, as shown in Figure 19. During the reaction, the organic phase containing dimethyltin dichloride in tetrahydrofuran solvent is added to a rapidly stirred aqueous solution of deprotonated diacid and polymerization occurred at the interface of the micelles formed. High molecular weight ($M_n \sim 6.5$–$9.3 \times 10^4$ g/mol) polymers are obtained as a result of the increased solubility of tin monomer in the organic phase.

Thermal stability ranges from 215 to 265°C. Aliphatic tin polyesters exhibit dielectric constants 5.3–6.6, and large bandgaps 4.7–6.7 eV, which is indicative of the high breakdown potential of the polymers, as shown in Figure 17 (63). When the number of methylene spacer is increased from one to three, there is a decrease in the dielectric constant and there is spike to the second maxima at six methylene spacer containing polymers as predicted by DFT. Majority of them exhibit losses on the order of $10^{-2}$ that is similar in magnitude as PE and PP. $p$(DMTSeb) with eight
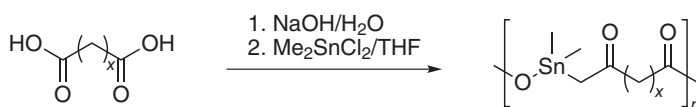


**Fig. 19.** Interfacial synthesis of poly(dimethyltin ester) from the Ref. 63.

methylene spacer in the repeat unit shows dissipation factor on the order of insulating polymers used in pulsed power application ($\sim 10^{-4}$) (63). Among these aliphatic systems, poly(dimethyltin glutarate) or $p$(DMTGlu), with three methylene spacers in the repeat unit, was considered as best dielectric material on the context of high dielectric constant and low dielectric loss. The experimental dielectric measurements strongly correlate with the DFT predictions of 3D organization of this polymeric system. Blends and copolymers of $p$(DMTSub) and $p$(DMTDMG) are also reported using increasing amounts of $p$(DMTSub) from 10 to 50% to find a balance between electronic properties and film morphology. Specific composition of blend and copolymer exhibit improved dielectric constants of 6.7–6.8 with dielectric losses of 1–2%. Higher energy density in copolymer 6 J/cm$^3$ is observed compared with 4 J/cm$^3$ for the blend due to the uniform distribution of diacid repeat units in the copolymer compared with the blend, leading toward improved film quality and subsequently high energy density (65).

The successful design of novel Sn-based polymers paved the path for an exploration of polymers containing various metals chosen from the periodic table. In Figure 18, DFT-computed results are presented for organometallic polymers constituted of (respectively) nine different metal atoms; also, shown for comparison are all the organics discussed in the previous section. The metal-based systems clearly surpass the pure organics in terms of high dielectric constants for given values of bandgap. This is owing to the enhanced polarity of chemical bonds (between electropositive metal atoms and highly electronegative atoms such as O, F, and Cl) in the organometallics, and the swinging and stretching of these polar bonds at low frequencies that cause fluctuations in polarization under electric fields (8,66).

## 6.  Some Limitations and Challenges

The use of inorganic ceramics as dielectric materials is a common practice due to their high dielectric constants, many into the thousands, which have been widely used in common electronic equipment such as multilayer ceramic capacitors (MLCC), for the last few decades. However, they suffer from high loss, low breakdown strength, and nongraceful failure modes (67). The widely used and low cost organic dielectric polymer, BOPP, has a remarkably low loss (tan$\delta$) of 0.0002 with a dielectric constant ($\varepsilon$) of about 2.25. However, BOPP is less than ideal for high temperature applications due to an increase in electronic conduction at temperatures above 85°C, requiring the capacitors to be extensively cooled in hotter environments (3). PVDF and derivatives of PVDF that have been discussed in previous sections, irrespective of their high dielectric constants and bandgaps, fluorine-containing polymers exhibit ferroelectric-type polarizations that are not desirable for high energy density applications (48,68,69). Organic polyimides, polythioureas (70), polyurethanes, and polyureas (43,71,72) have also been studied recently for dielectric applications, but suffer from difficulty in processing, thermal limitations, and increased loss compared with BOPP. Recently, BaTiO$_3$ nanoparticles have been dispersed on ferroelectric polymers to increase the overall dielectric constant, with improved energy densities over the ferroelectric polymer

alone. However, incorporation of nanoparticles into polymer networks leads to aggregation on the nanoparticles and limits the field penetration in the inorganic phase (73). To overcome this issue, researchers have created layered structures of PVDF and $BaTiO_3$ nanoparticles and nanofibers in a sandwiched structure to help improve the breakdown of the resulting films (74). Another limitation in PVDF films is due to their conduction losses within the films. It has been found that incorporation of alumina nanofillers can create traps that reduce mobile carrier concentration leading to conduction loss (75). Additional nanoparticles and their corresponding challenges with incorporating into the polymer matrix have been explored further by Chen and co-workers (76).

Component properties like dielectric constant, dielectric breakdown field, dielectric loss, defect content (and their effects), electronic structure, glass transition and melting temperatures, polymer morphology and rheology, intrinsic thermal conductivity, and so on have their own challenges. These components areas are dependent on each other, and improvement in one component has a significant effect on others. Properties such as thermal management need to improve in parallel with increased dielectric constant and certainly cannot compensate on dielectric loss. While a general solution that meets the needs of all high energy density applications may not exist, any improvement over the present technology for specific applications must be consistent with majority of the materials-specific needs, that is, new materials must be evaluated in the context of likely applications.

## CITED PUBLICATIONS

1. R. Coelho, *Physics of Dielectrics for the Engineer*, Elsevier, 2012.
2. Omar, *Elementary Solid State Physics*, Pearson Education India, 1999.
3. M. Rabuffi and G. Picci, *IEEE Trans. Plasma Sci. IEEE Nucl. Plasma Sci. Soc.* **30** (5), 1939–1942 (2002).
4. H. S. Nalwa, *Handbook of Low and High Dielectric Constant Materials and Their Applications*, Academic Press, 1999.
5. A. F. Baldwin and co-workers, *Adv. Mater.* **27** (2), 346–351 (2015).
6. H. Chen and co-workers, *Prog. Nat. Sci.* **19** (3), 291–312 (2009).
7. X. Hao, *J. Adv. Dielectr.* **3** (1), 1330001 (2013).
8. T. D. Huan and co-workers, *Prog. Mater. Sci.* **83**, 236–269 (2016).
9. S. Cygan and J. R. Laghari, *IEEE Trans. Elect. Insul.* **EI-22** (6), 835–837 (1987).
10. L. Zhu, *J. Phys. Chem. Lett.* **5** (21), 3677–3687 (2014).
11. J. L. Nash, *Polym. Eng. Sci.* **28** (13), 862–870 (1988).
12. E. W. Anderson and D. W. McCall, *J. Polym. Sci.* **31** (122), 241–242 (1958).
13. T. Umemura, T. Suzuki, and T. Kashiwazaki, *IEEE Trans. Elect. Insul.* **EI-17** (4), 300–305 (1982).
14. T. Umemura, K. Akiyama, and D. Couderc, *IEEE Trans. Elect. Insul.* **EI-21** (2), 137–144 (1986).
15. A. A. Benderly and B. S. Bernstein, *J. Appl. Polym. Sci.* **13** (3), 505–517 (1969).
16. H. M. Banford and co-workers, *IEEE Trans. Dielectr. Electr. Insul.* **3** (4), 594–598 (1996).
17. P. Huo and P. Cebe, *J. Polym. Sci. B Polym. Phys.* **30** (3), 239–250 (1992).
18. L. Qi, L. Petersson, and T. Liu, *J. Int. Council Electr. Eng.* **4** (1), 1–6 (2014).

19. L. N. Ji, *Appl. Mech. Mater.* **312**, 406–410 (2013).

20. J. Ulrych, R. Polansky, and J. Pihera, Dielectric analysis of polyethylene terephthalate (PET) and polyethylene naphthalate (PEN) films, *Proceedings of the 2014 15th International Scientific Conference on Electric Power Engineering (EPE)*, 2014, 411–415.

21. M. El-Shabasy and A. S. Riad, *Physica B Condens. Matter* **222** (1–3), 153–159 (1996).

22. Y. Aoki and J. O. Brittain, *J. Polym. Sci. Polym. Phys. Ed.* **14** (7), 1297–1304 (1976).

23. J. Pan, and co-workers, *Appl. Phys. Lett.* **95** (2), 022902 (2009).

24. T. W. Giants, *IEEE Trans. Dielectr. Electr. Insul.* **1** (6), 991–999 (1994).

25. W. A. Walls and co-workers, *IEEE Trans. Magn.* **35** (1), 262–267 (1999).

26. F. Beach and I. McNab, Present and Future Naval Applications for Pulsed Power, *2005 IEEE Pulsed Power Conference*, 2005.

27. Quan Li and P. Wolfs, *IEEE Trans. Power Electron.* **23** (3), 1320–1333 (2008).

28. V. Sharma and co-workers, *Nat. Commun.* **5**, 4845 (2014).

29. A. Mannodi-Kanakkithodi and co-workers, *Adv. Mater.* **28** (30), 6277–6291 (2016).

30. S. Wu and co-workers, *J. Electron. Mater.* **43** (12), 4548–4551 (2014).

31. A. F. Baldwin, and co-workers, *J. Appl. Polym. Sci.* **130** (2), 1276–1280 (2013).

32. S. Chisca, I. Sava, V.-E. Musteata, and M. Bruma, Dielectric and Conduction Properties of Polyimide Films, *CAS 2011 Proceedings (2011 International Semiconductor Conference)*, 2011, 253–256.

33. D. H. Wang and co-workers, *J. Polym. Sci. A Polym. Chem.* **53** (3), 422–436 (2015).

34. R. Ma and co-workers, *ACS Appl. Mater. Interfaces* **6** (13), 10445–10451 (2014).

35. W. D. Kumler and G. M. Fohlen, *J. Am. Chem. Soc.* **64** (8), 1944–1948 (1942).

36. N. Yamazaki, T. Iguchi, and F. Higashi, *J. Polym. Sci. Polym. Chem. Ed.* **17** (3), 835–841 (1979).

37. L. Alexandru and L. Dascălu, *J. Polym. Sci.* **52** (157), 331–339 (1961).

38. S. Mallakpour and H. Raheno, *J. Appl. Polym. Sci.* **89** (10), 2692–2700 (2003).

39. X.-S. Wang and co-workers, *Jpn. J. Appl. Phys.* **34** (3R), 1585 (2014).

40. Y. Wang and co-workers, *Appl. Phys. Lett.* **94** (20), 202905 (2009).

41. X.-S. Wang and co-workers, *Jpn. J. Appl. Phys.* **33**, 5842–5847 (1994).

42. R. G. Lorenzini and co-workers, *Polymer* **54** (14), 3529–3533 (2013).

43. S. Wu and co-workers, *Appl. Phys. Lett.* **104** (7), 072903 (2014).

44. S. Wu and co-workers, *Adv. Mater.* **25** (12), 1734–1738 (2013).

45. R. Ma and co-workers, *J. Mater. Chem. A Mater. Energy Sustain.* **3** (28), 14845–14852 (2015).

46. G. Odian, *Principles of Polymerization*, John Wiley & Sons, Inc. 2004.

47. A. Mannodi-Kanakkithodi and co-workers, *Adv. Mater.* **28**, 6277–6291 (2016).

48. Y. Wang and co-workers, *IEEE Trans. Dielectr. Electr. Insul.* **17** (4), 1036–1042 (2010).

49. R. Gregorio Jr. and E. M. Ueno, *J. Mater. Sci.* **34** (18), 4489–4500 (1999).

50. W. Li and co-workers, *Appl. Phys. Lett.* **96** (19), 192905 (2010).

51. F. Bauer and co-workers, *IEEE Trans. Dielectr. Electr. Insul.* **11** (2), 293–298 (2004).

52. S. Baroni and co-workers, *Rev. Mod. Phys.* **73** (2), 515 (2001).

53. X. Gonze, *Phys. Rev. B Condens. Matter* **55** (16), 10337 (1997).

54. J. Heyd, G. E. Scuseria, and M. Ernzerhof, *J. Chem. Phys.* **118** (18), 8207–8215 (2003).

55. J. P. Perdew, *Int. J. Quantum Chem.* **28** (S19), 497–523 (2009).

56. A. Mannodi-Kanakkithodi and co-workers, *Sci. Rep.* **6**, 20952 (2016).

57. M. Amsler and S. Goedecker, *J. Chem. Phys.* **133** (22), 224104 (2010).

58. G. M. Treich and co-workers, *IEEE Trans. Dielectr. Electr. Insul.* **24** (2), 732–743 (2017).

59. A. Mannodi-Kanakkithodi, C. C. Wang, and R. Ramprasad, *J. Mater. Sci.* **50** (2), 801–807 (2014).

60. C. C. Wang, G. Pilania, and R. Ramprasad, *Phys. Rev. B Condens. Matter* **87** (3), 035103 (2013).

61. H. Furukawa and co-workers, *Science* **341** (6149), 1230444 (2013).

62. G. Pilania and co-workers, *J. Chem. Inf. Model.* **53** (4), 879–886 (2013).
63. A. F. Baldwin and co-workers, *Macromolecules* **48** (8), 2422–2428 (2015).
64. A. F. Baldwin and co-workers, *Macromol. Rapid Commun.* **35** (24), 2082–2088 (2014).
65. G. M. Treich and co-workers, *ACS Appl. Mater. Interfaces* **8** (33), 21270–21277 (2016).
66. T. D. Huan and co-workers, *Sci. Data* **3**, 160012 (2016).
67. J. Ho, T. R. Jow, and S. Boggs, *IEEE Electr. Insul. Mag.* **26** (1), 20–25 (2010).
68. B. Chu and co-workers, *Science* **313** (5785), 334–336 (2006).
69. Q. M. Zhang, *Science* **280** (5372), 2101–2104 (1998).
70. Q. Burlingame and co-workers, *Adv. Energy Mater.* **3** (8), 1051–1055 (2013).
71. Z. Cheng and co-workers, *Appl. Phys. Lett.* **106** (20), 202902 (2015).
72. Y. Thakur and co-workers, *J. Electron. Mater.* **45** (10), 4721–4725 (2016).
73. T. Zhou and co-workers, *ACS Appl. Mater. Interfaces* **3** (7), 2184–2188 (2011).
74. P. Hu and co-workers, *Adv. Funct. Mater.* **24** (21), 3172–3178 (2014).
75. Y. Thakur, M. H. Lean, and Q. M. Zhang, *Appl. Phys. Lett.* **110** (12), 122905 (2017).
76. Q. Chen and co-workers, *Annu. Rev. Mater. Res.* **45** (1), 433–458 (2015).

SHAMIMA NASREEN [iD]
GREGORY M. TREICH
MATTHEW L. BACZKOWSKI
ARUN K. MANNODI-KANAKKITHODI
YANG CAO
RAMAMURTHY RAMPRASAD
GREGORY SOTZING
University of Connecticut, Storrs, CT, USA